Synthesis and Characterization of Erbium and Neodymium Oxide doped Titanium Oxide Nanocomposites and their Application in Visible Light Photocatalysis of Congo Red.

BY

DANIEL N. ALOTSI (DNA)

A project report submitted in partial fulfillment of the requirements for completion and the award of degree in:

BACHELOR OF SCIENCE IN CHEMICAL TECHNOLOGY

(B.Sc. Chem. Tech.)

THE NATIONAL UNIVERSITY OF LESOTHO

Faculty of Science and Technology

Department of Chemistry and Chemical Technology

Supervisor: Prof. Hailmichael Alemu

DECLARATION

I hereby verify that this document and the analogy made in it has been done by me (Daniel Ntjamang Alotsi (DNA)). No parts of this project have been copied with the exception of external information acknowledged by references.

Signature: _____

Place and Date: _____

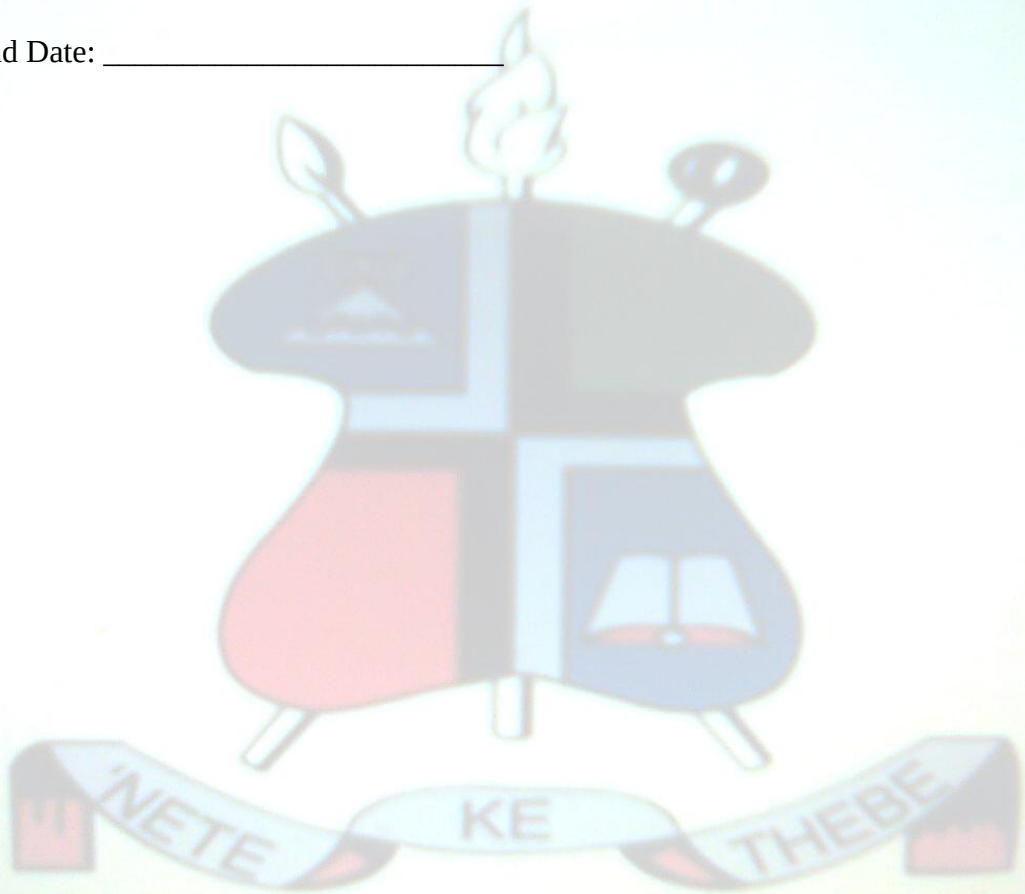

DEDICATION

May I dedicated the success of this work to my Uncle's entire family and my sister, people who never gave up in my straggle through the entire journey in school, for the support they gave to me and their exceedingly excellent motivation during harsh times. May peace and truth reign wherever I go and whenever I meet those who have been by my side. Peace, Love and Harmony to all humankind!

Daniel Ntjamang Alotsi (DNA)

NUL, Roma, May 2011

ACKNOWLEDGEMENTS

May I thank my uncle's entire family (Mr and Mrs Mokobori) and my sister (Mrs Lillian Mokobori) for the overall support they gave me through the entire journey from High school up to Tertiary level; I am really blessed to have had people like you in my life. With great contentment, I am also gratified to have had Prof. Hailmichael Alemu as my supervisor, for the excellent supervision, providing me with necessary equipments and making necessary comments through the entire project. My special thanks goes to Mr. Macheli Lebohang for the guidance he gave me in laboratory sessions; the Department of Geography and Physics (NUL) for allowing me use their equipments. May I also thank the entire department of Chemistry and Chemical Technology allowing me to grow in academically and withstand challenges of being a Student.

I also exude with pride to have gone through this Journey with humorous and hard working course mates (CTEC 4th year candidates 2010/2011) who have been friends indeed.

ABOVE ALL GLORY IS TO ALMIGHTY GOD WHO ALWAYS STRENGTHENS ME!

ABSTRACT

Nanocomposites (NCs) of Titanium dioxide doped with Erbium and Neodymium oxides, ($TiO_2[Er_2O_3]_x$ and $TiO_2[Er_2O_3]_x$, x=0.1,0.2) were prepared both by chemical co-precipitation followed by hydrolysis (CPH) as well as the solid-state reaction (SSR). The CPH synthesized NCs were obtained with particle sizes in the range (10nm-30nm). TiO_2 was also synthesized using precipitation followed by hydrolysis method. All the NCs were investigated for their capability of degrading a dye, Congo Red (CR) using visible light and about 99.6% of CR was degraded. Throughout the entire research, all the chemically synthesized NCs showed high photocatalytic activity and this is attributed to smaller particle size of the NCs as compared to those NCs prepared by the SSR method. This directly reflects that photosensitization is major route of photocatalytic degradation mediated on TiO_2 NCs. On comparison with the synthesized TiO_2, the doped NCs revealed no greater photocatalytic activity than the synthesized TiO_2, however this is apparent since TiO_2 was synthesized with similar method to CPH method.

Table of Contents

TABLE OF FIGURES

1.0 INTRODUCTION

Discharge of untreated waste products into the environments is the worldwide problem which is of great concern today since waste products on environments; whether solid or non-solid influence the natural processes of the ecosystem [1]. Nevertheless, the discharge of waste on environments reveal negative impacts on human's life comfort due to their various levels of toxicity, leading to disease causing agents as well as affecting the food chain in the ecosystem. The most undesirable end is that almost all waste products especially the water-soluble ones end up in water systems. Currently the coloration of water in rivers and streams arise from the large amounts of colored organic effluents (mainly the synthetic dyes) discharges from industries such as textile, rubber, cosmetic, paper industries etc, where coloration of products is of great importance [1] hence such industries are the major contributors to environmental pollution. The main environmental impacts caused by these industries involve their high water consumption which may be used as a coolant, cleaning agent or solvent, for instance about 80–100 L kg^{-1} of cotton is reported in the case of textile industry. Nevertheless, the low fixation degree of raw materials, such as starching agents, detergents, dyes and other materials is yet another factor which aggravates pollution [2]. These two situations lead to the generation of large volumes of wastewaters containing high organic loads and strong color [3].

It is reported that more than 60% of the dyes of the world production is utilized in textile industries of which during the processing of textiles, about 10% -20% are discharged as effluents [1, 4]. Discharge of dye effluents into water resource distract the food web in water due to the fact that their intense color reduce the light transmission in water thereby inhibiting the growth of most aquatic plants as well as raising the biological oxygen demand (BOD) and the chemical oxygen demand (COD) in water. These may lead to suffocation of animals which cling on dissolved oxygen in water for their survival and consequently the aquatic life ultimately extinguish [4, 5]. Despite the fact that dyes raise the BOD of water, even in small amounts they are also known to have potential to cause allergenic dermatitis and skin irritation and some are also known to be carcinogenic and mutagenic for most aquatic organisms [5].

Dyes are categorized into three broad groups namely; cationic, non-ionic and anionic dyes. Due to their negative impacts to man, animals and water used daily for domestic purposes, discharges of dye effluents require a special handling as well as proper and effective treatments; such treatments are not only vital for the possible reuse of disinfected water but also for the sake of healthier and cleaner environment [6].

1.2 CONGO RED (CR)

Among the most largely consumed dyes, azo-dyes are the most commonly utilized reagents due to the fact that they possess an azo-group which confers to these chemicals a certain resistance to light, oxygen ,acids and bases, the desired properties for clothes' makers[4]. CR dye is one of important anionic azo-dyes (synthesized by Paul Bottiger, 1883 in Germany) [7]. It is a colored organic dye with a complex chemical structure and high molecular weight (molecular weight: 696.66 g/mol; formula: $C_{32}H_{22}N_6Na_2O_6S_2$). The chemical structure is the sodium salt of benzidinediazo-bis-1-naphtylamine-4-sulfonic acid [7, 4]. The dye's chemical structure is shown in Fig.1.

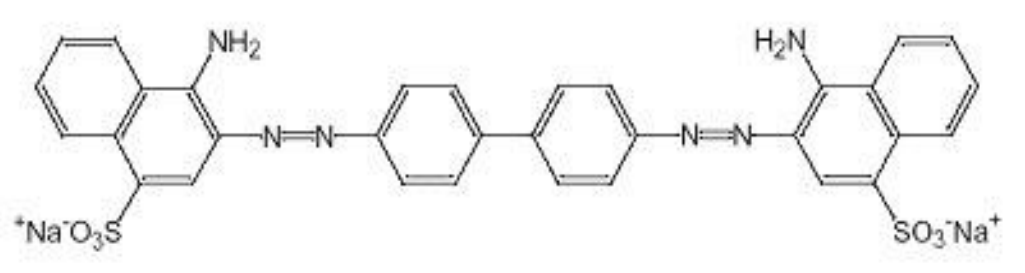

Figure 1: Chemical structure of the studied molecule of Congo Red

.

CR is characterized by high solubility in organic solvents such as ethanol and moderate solubility in water and is highly persistent in the environment, once discharged into a natural environment. The use of CR in cotton textile, wood pulp and paper industries has long been abandoned mainly

due to its toxicity and its tendency to alter color when it gets in contact with sweat [7]. However, the study of the degradation of CR is an interesting one, not only for being possible pollutant of industrial effluents but also because it is a good representative of complex pollutants [8].

Though it is banned in industry as dyeing agent, CR still has some useful properties. For instance it can be used as a pH indicator due to its ability to exhibit a color change from blue to red at pH 3.0-5.2 and it is an important chemical in biochemistry and histology where it is used to stain microscopic samples for academic purposes [7].

1.3 LITERATURE REVIEW

Various methods have been developed and are endeavoring to reduce as well as to eliminate the discharge of wastewaters containing dye effluents into the environments. These methods fall into three broad categories known as physical, chemical and biological (biodegradation) methods. Physical methods such as absorption of CR on powdered activated carbon (PAC) and granular activated carbon (GAC) are already reported [1]. Chemical methods such as removal of CR from textile wastewaters by ozonation as well as by TiO_2-zeolite photo-degradation are also reported to be adequate [4, 9]. Chlorination is also a well known chemical method for disinfecting water.

Current pretreatment are large, they have little or no economical advantage other than the elimination or reduction of sewer charges, and consequently companies are reluctant to adopt such treatment methods simply out of concern of reducing the environmental pollution. They might do so mainly to cut costs or to generate extra revenue [5]. Some traditional methods which are known to be effective in de-colorization of pollutants use more energy as well as chemicals and could potentially give rise to toxic chemicals in effluents through degradation or alteration of the conjugated systems of dyes [10].

Photocatalytic degradation of organic pollutants based on semiconductor photochemistry (also known as advanced oxidative process) has been another attractive method since 1970s and in recent years this method is being investigated for degrading synthetic dyes. The most effective photocatalyst for this purpose is titanium oxide (TiO_2) which is further studied in this project.

Along this line, nanoparticles of TiO_2 doped with ferric iron as well as those doped with $ZnFe_2O_4$ (TZF) and yttrium (TY) have well been researched and documented for the sole purpose of degrading industrial effluents (basically dye effluents) [4,11,12] . In this project further work is done to exploit further the capability of doping TiO_2 with other potentially capable semiconductors to enhance the Photocatalytic activity of TIO_2 for the purpose of degrading organic pollutants, the dopants being oxides of Erbium and Neodymium.

1.4 PRINCIPLES OF PHOTOCATALYSIS

Photocatalysis may be defined briefly as the acceleration of a photoreaction in the presence of a catalyst by direct irradiation of a catalyst which results in the lowering of the activation energy therefore enabling primary reaction to occur. The process involves the initial absorption of photons by a molecule or the catalyst substrate in order to produce highly reactive electronically exited states [13]. In heterogeneous photocatalysis system, also known as photocatalytic oxidation (PCO), photo-induced molecular reactions or transformations occur at the surface of a catalyst. Depending on where the first excitation takes place, photocatalysis can be split into two fundamental processes, namely the catalyzed photoreaction and sensitized photoreaction. The latter takes place when the initial photoexitation occurs in an adsorbate molecule which in turn interacts with the ground state of the catalyst substrate while the former refers to photocatalysis when the initial excitation takes place in the catalyst substrate followed by electron or energy transfer from the photoexited catalyst into a ground state molecule [14, 15, 16].

1.5 MECHNISMS IN TIO_2 PHOTOCATALYSIS

Fujishima and Honda discovered the splitting of water on TiO_2 electrodes in 1972. This discovery marked the beginning of new era in heterogeneous photocatalysis. Since then, chemists, physicists as well as chemical engineers conducted researches in understanding the fundamental processes and enhancing the photocatalytic efficiency of TiO_2 [17].

TiO_2 is a wide band gap (3.2 eV) semiconductor with several attractive optical and electronic properties; as a result it plays a fundamental role as a photocatalyst in nanotechnology [6]. When a photocatalyst is irradiated with ultraviolet (UV) radiations of suitable wavelengths (correspond to 388 nm for TiO_2) from either sunlight or illuminated light source, (e.g. fluorescent lamp). The electrons in the valence band (VB) of this semiconductor get exited and their excess energy promotes the electrons into the conduction band (CB) and consequently creating negative-electron and positive holes (e-/h+) pairs. This state is referred to as the semiconductor photo-exitation. The generated (e-/h+) pairs are the most important features which initiate the primary reactions to take place by reacting with the hydroxide ions, water and oxygen to form highly active species (e.g. the hydroxyl radicals OH* and superoxide radical anions O_2^-) which interact directly with the pollutants leading to their degradation[7,8,9]. Among the generated radicals, the positive holes (h+) and the hydroxyl radicals are the most influential radicals in photocatalytic oxidation process [10]. In this mechanism the band gap of a photocatalyst is a controlling factor. The following are the possible reaction equations that lead to the degradation of an organic pollutant through the photo-exitation mechanism on TiO2 particle.

$TiO_2 + \text{light } (h\nu) \rightarrow TiO2\ (e^-_{CB} + h^+_{VB})$ ..... (1)

$TiO_2 + H_2O\text{ads} \rightarrow TiO_2 + OH^- + H^+$ ..... (2)

$e^-_{CB} + O_{2ads} \rightarrow O^{2-}$ ..... (3)

$h^+_{VB} + OH^- \rightarrow OH^*$ ..... (4)

$OH^* + \text{Organics} \rightarrow H_2O + CO_2 + \text{mineral acids}$..... (5)

The other equally important mechanism is the photosensitization. In this process, the pollutant molecule (e.g. dye molecule) must initially adsorb onto the surface of the catalyst (semiconductor) and start absorbing visible radiations. This eventually results to the electrons of the adsorbate molecule being photochemically exited and finally transferred to the particle of a catalyst. This transfer produces superoxide anion radicals from reduction of molecular oxygen and a cation radical is also produced from the pollutant molecule hence leading to the degradation of other pollutants. In this case the degradation of the organic pollutant is entirely dependent on the effective surface area of the catalyst particle [11].

It must be borne in mind that both photosensitization and photo-exitation mechanisms may take place simultaneously and which mechanism dominates depend on the chemical and adsorption properties of the pollutant as well as the surface chemistry of the catalyst, thus catalyst particle's properties such as surface area, porosity, crystal phase, structure, particle size as well as presence of dopants play a fundamental role in photocatalysis hence they influence to a greater extend, the photocatalytic activity and performance of TiO_2 in photocatalysis.

1.51 Enhancement of photocatalytic efficiency

It is clear from section 1.5 therefore that the photocatalytic performance of a photocatalyst is dependent on its band gap as well as the particle size. However various factors need also be considered since may also contribute to the photocatalytic efficiency of the catalyst (semiconductor). For instance TiO_2 exist in various phases that possess different properties to be utilized in nanotechnology, the well known crystal phases being the rutile phase and the anatase form. Studies on these phases indicate that the rutile phase can be photo-activated by visible light but that is accompanied by deleterious electron-hole pair (EHP) recombination hence this may lead to reduced photocatalytic performance due to limited reaction time. On the other hand the anatase form can only be exited by UV light hence to optimize the overall efficiency; it is legitimate therefore to synthesize a mixed phase photocatalyst [18].

1.52 Particle size optimization and band gap modification

Particle size as well as band gap are believed to be the leading factors influencing the photocatalytic efficiency of a semiconductor as observed in section 1.5. Smaller particles increase the surface area for absorption of pollutants on the catalyst surface hence this enhance the reactions through photosensitization mechanism and in several cases optimum conditions were found be confined to particles having sizes within 10nm to15nm [19], however various authors indicate that particles size need not be too small, that is less than 10nm since this may accelerate the impact of rapid EHP re-combination leading to decreased activity of the catalyst, in addition smaller particle size may generate wider band gaps due to quantum size effect and

consequently cutoff wavelengths (λ_{cutoff}) may blue-shift thereby shifting the regions of the spectrum more towards smaller wavelength than the useful visible regions[12].

The band gap is another important factor since the ability of photo-exited electrons to reach the conduction band is dependent on the energy absorbed as well as the separation between the bands of a semiconductor. It has been reported that band gap can be narrowed through doping and along this line nanoparticles of TiO_2 doped with some transition metals [6, 11, 20] as well as some semiconductor doped nanocomposites [11, 12] have been documented.

1.0 PROJECT OBJECTIVES

The aim of this project is to synthesize and characterize nanocomposites (NCs) of TiO_2 doped with oxides of Erbium and Neodymium and to finally use them as photocatalyst for the degradation of the pollutants, specifically the synthetic dye Congo Red (CR). An ideal photocatalyst should meet the following requirements; it should be a non-hazardous substance, recoverable, should be having high photochemical stability and be cost effective.

The major purposes will be to compare the performance of the NCs on degradation of CR and to evaluate necessity of doping TiO_2 with the rare earth metals used. Since particles are to be synthesized with varying contents of doping materials as well as different methods and are expected to exhibit different photocatalytic performance towards the degradation of CR dye. It is vital therefore to degrade equal concentrations of the CR dye with equal amounts of different nanoparticles at unchanging conditions in order to evaluate the performance of all the synthesized particles.

2.1 Toxicity reduction

In this work the goal is to degrade a pollutant, hence it is also vital to consider using environmentally benign materials so that solving one problem does not create five more. The use of TiO_2 is adopted in this study since it is a non-toxic material; in fact this compound is a constituent of toothpastes and many cosmetics which are day to day useful substances. This makes TiO_2 a useful material in this study aside from being a stable photocatalyst and a capable material to degrade wide variety of organic pollutants.

2.2 Cost effectiveness

Industries and companies are profit making organizations; as a result they may not get interested in adopting or implementing cleaner technological methods which are non-economical for the sake of safeguarding the environment. It is therefore important to consider the feasibility in terms of economy for such technologies while developing methods that lead to degradation of pollutants; this reflects that methods being developed should be as economical as possible to attract organizations to contribute positively in the world endeavors to minimize as well as to eliminate contaminants. The method of degrading pollutants with TiO_2 nanoparticles is indeed a promising one in terms of monetary issues since this substance is readily available with affordable prices.

2.3 photochemical stability

Ideal photocatalyst should be photochemically stable and therefore insusceptible to any type of corrosion in wide range of dynamic reaction environments. This therefore increases the lifetime of a photocatalyst as well as minimizing the cost of catalyst replacement from time to time hence a good semiconductor photocatalyst should sustain constant performance under different reaction condition.

3.0 EXPERIMENTAL

3.1 MATERIALS

Neodymium nitrate hex hydrate, $Nd(NO_3)_3.6H_2O$ (99.9% metal basis), erbium nitrate pent hydrate, $Er(NO_3)_3.5H_2O$ (99.9% metal basis), isopropanol (ASSAY 99%) and titanium (IV)butoxide, $Ti(OBu)_4$ (97% reagent grate) were the reagents of the Aldrich chemical corporations while ammonium hydroxide (ASSAY 25%) was the reagent of Shalom laboratory supplies. Congo red was the product of E. Merck co, (Darmstadt, Germany).

3.2 SYNTHESIS PROCESS

Neodymium oxide and Erbium oxide doped titanium oxide nanocomposites (NCs) $TiO_2[M_2O_3]_{x,}$ x = 0.1 and 0.2 (M=Nd or Er) were synthesized using two preparation methods reported in literature [12]. The methods of synthesis utilized were, co-precipitation followed by hydrolysis (CPH) and solid state reaction (SSR). The CPH method, initially involved the nitrate salt of each metal dissolution in isopropanol through stirring and heating at around 55-65^oC. 3.5M ammonium hydroxide (NH_4OH) was prepared in isopropanol and 10ml of this solution was added to the solution of metal nitrate to affect hydrolysis. This raised the PH of the metal nitrate solution to around PH 6.5 where the nitrate precursors were precipitated. Approximately 10ml of distilled water was added drop wisely to the solution and the solution was further agitated for 30 minutes.

A mixture of $Ti(OBu)_4$ and isopropanol was prepared in the ratio of 1:2 by weight and added drop wisely to the co-precipitated metal nitrate precursor for controlled hydrolysis and agitation of the mixture was continued for 60 minutes while slowly adding distilled water to prevent the setting of the solution. The doped NCs were then recovered from the solution by drying at room temperature followed by calcinations at 400^oC for a maximum period of three hours. Fig.2 illustrates the chemical synthesis for Erbium and Neodymium oxide doped TiO_2 NCs. TiO_2 was also synthesized following the same procedure as in Fig.2; however the only difference is that no metal nitrate was dissolved in isopropanol.

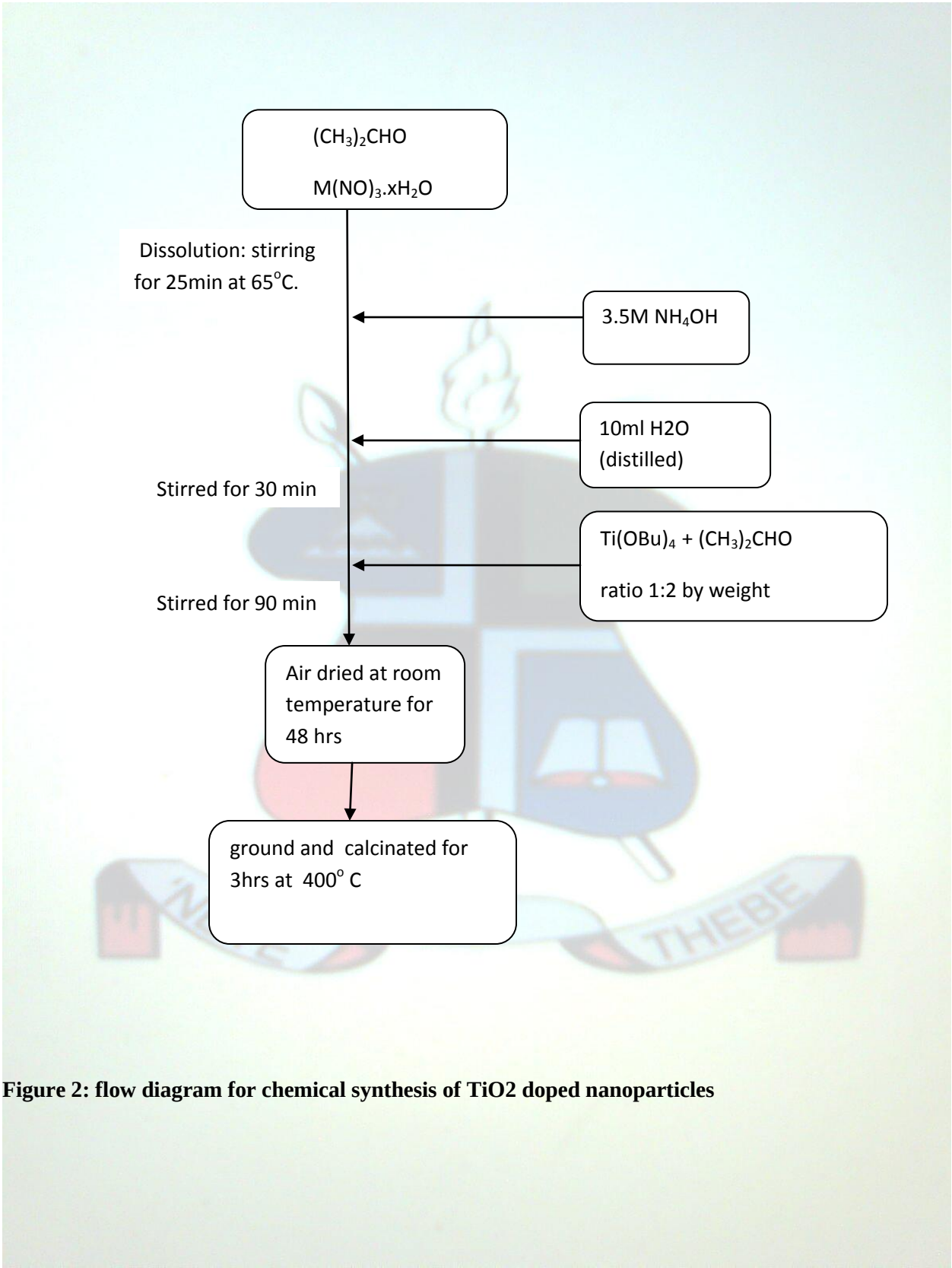

Figure 2: flow diagram for chemical synthesis of TiO2 doped nanoparticles

TiO_2 NCs were also synthesized with the SSR method. This involved dissolution of the metal nitrates in isopropanol followed by small additions of commercial TiO_2 to the required amount while continuously stirring. The molten solution was then further agitated, dried, ground and calcinated for 3 hours at 400 ^oC. The following Fig: 3 illustrate details of SSR method for NCs synthesis.

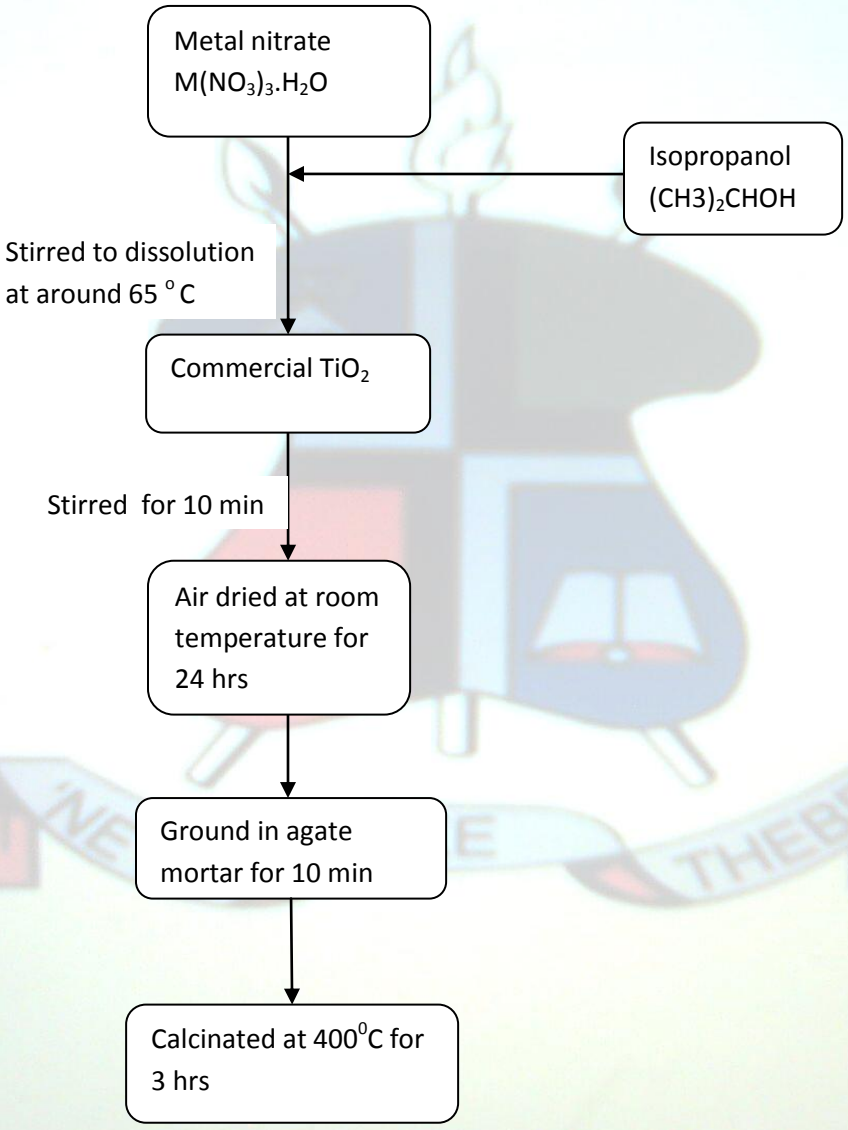

Figure 3: Flow diagram for synthesis of Nanoparticles by solid-state reaction method (SSR)

3.3 MEASUREMENTS

Powder x-ray diffraction (XRD) was used to characterize the samples obtained from the synthesis procedures (section 3.2), in this part the measurements of undoped TiO_2 and as well as for pure oxides of Erbium and Neodymium were performed. The XRD of the powdered samples was carried out on a Shimadzu D6000 diffractometer (Shimadzu, Japan) using Cu Kα radiation (λ = 1.5406 A°). Particle size measurements of the NCs were taken using Transmission Electron Microscope (TEM). All the measurements of particle size were taken at the highest resolution of this instrument.

The visible-light photocatalytic activity was carried out using a cost efficient photoreactor organized in the laboratory (Fig.4 shows the schematic diagram of the photoreactor). In this scheme, a one liter glass beaker with a magnetic stirring bar was placed on a magnetic stirrer. A 250 ml beaker was placed inside it that separated the light source (fluorescent lamp) from the water. The 250ml was held in place inside the 1L beaker using a ring attached to a ring stand fitted on the top. After addition of 750 ml of 5.5mg/l of dye solution and the photocatalyst (250mg/L) to the solution, the 250ml beaker glass was sealed with parafilm where it touched the top outer rim of the large beaker. A 60 W fluorescent lamp (Phillips), held in place with a three pronged clamp was finally placed in the middle of the 250ml beaker in the dye solution so that it was not touching the sides and the bottom of the 250ml beaker. Before the start of photocatalysis experiments, the amounts of photocatalyst and the experimental solution of dye were optimized for best results. Accordingly, an experimental solution (750 ml) containing 5.5 mg/l of Congo red, a stirring bar, and 250 mg/l of photocatalyst sample were placed in the photoreactor and the fluorescent lamp was turned on. The solution was stirred throughout the duration of the experiment. At predetermined times (after every 30 minutes up to 180 minutes); 3ml aliquots of the dye solution were taken from the photoreactor and centrifuged for about 3min. The absorbance of the centrifuged solution was measured and recorded at wavelengths in the range, λ= 496-499nm using a UV-VIS Shimadzu model 1201 spectrophotometer coupled with a computer. In the entire photocatalysis experiments for all the prepared NC samples, the instrument was baseline corrected with distilled water. For a better analysis of the results, for every solution from the centrifuge, the entire useful UV-visible region (600nm-400nm) within

which the absorption peak for CR is found was scanned and the degradation peak curves were obtained.

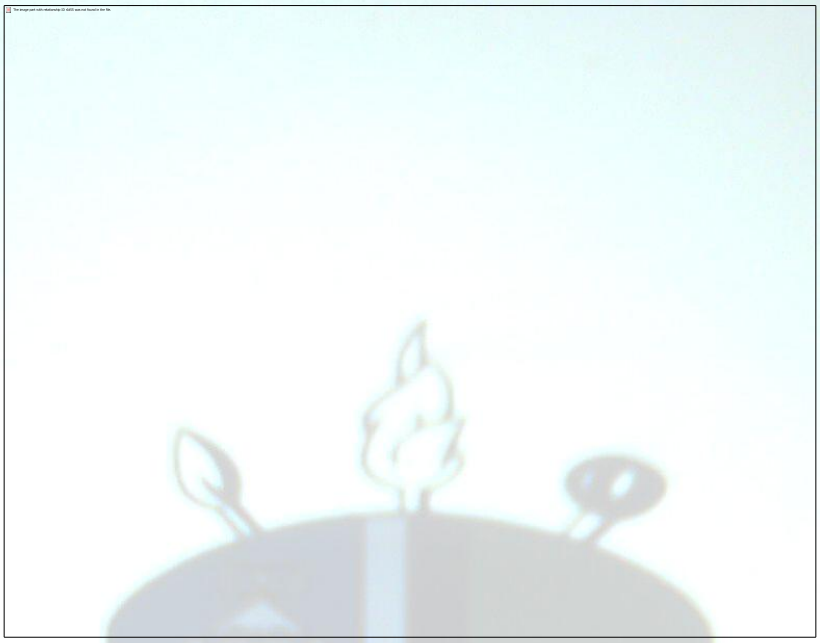

Figure 4: A schematic representation diagram (not to scale) of the photoreactor used.

4.0 RESULTS AND DISCUSIONS

4.1 particle size analysis

As indicated from section 3.3, the analysis for particle sizes was performed using Transmission Electron Microscope (TEM) operating at high resolution. Particle sizes of the prepared NCs were found to be in the range (10-30nm) rough. Fig: 2 below indicates a typical TEM image of one of the CPH synthesized NCs ($TiO_2[Nd_2O_2]_{x=0.1,0.2}$).

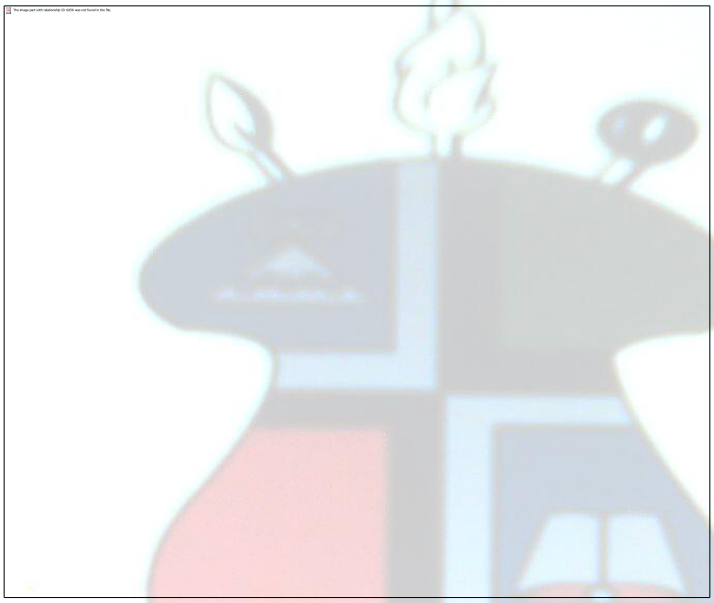

Figure 5: Typical TEM image for one of the prepared NCs.

The initial observation suggests that the particles are very small as was desired to obtain optimal particle sizes. The smaller particle sizes enable enhanced adsorption due to increased surface area and consequently this is likely to yield high degradation of the dye [19].

4.2: X-Ray Diffraction of Rare Earth doped TiO_2 Nanocomposites

4.21: XRD analysis of prepared nanocomposites.

The Fig: 6 below show x-ray diffraction (XRD) pattern results for the oxides of Erbium and Neodymium doped TiO_2 ($TiO_2[M_2O_3]_{x=0.1,0.2}$) NCs samples prepared by CPH method. For

comparison, the XRD results for pure TiO_2 as well as pure oxides of Erbium and Neodymium are also shown. The crystalline powders of TiO_2, Er_2O_3 and Nd_2O_3 show sharp peaks as expected indicating pure samples. However, in the XRD patterns for the composites prepared by chemical synthesis, the peaks are less intense and spread (larger FWHM (full width at half maxima) as compared to the patterns of pure oxides). This observation directly indicates the formation of particles with very small size, which is confirmed by the TEM pictures, which shows particle size ranges between 10 – 30 nm. With the increasing value of *x* in these samples, a gradually decreasing amount of TiO_2 is revealed by the decreasing heights of the corresponding peaks indicating the effectiveness of doping.

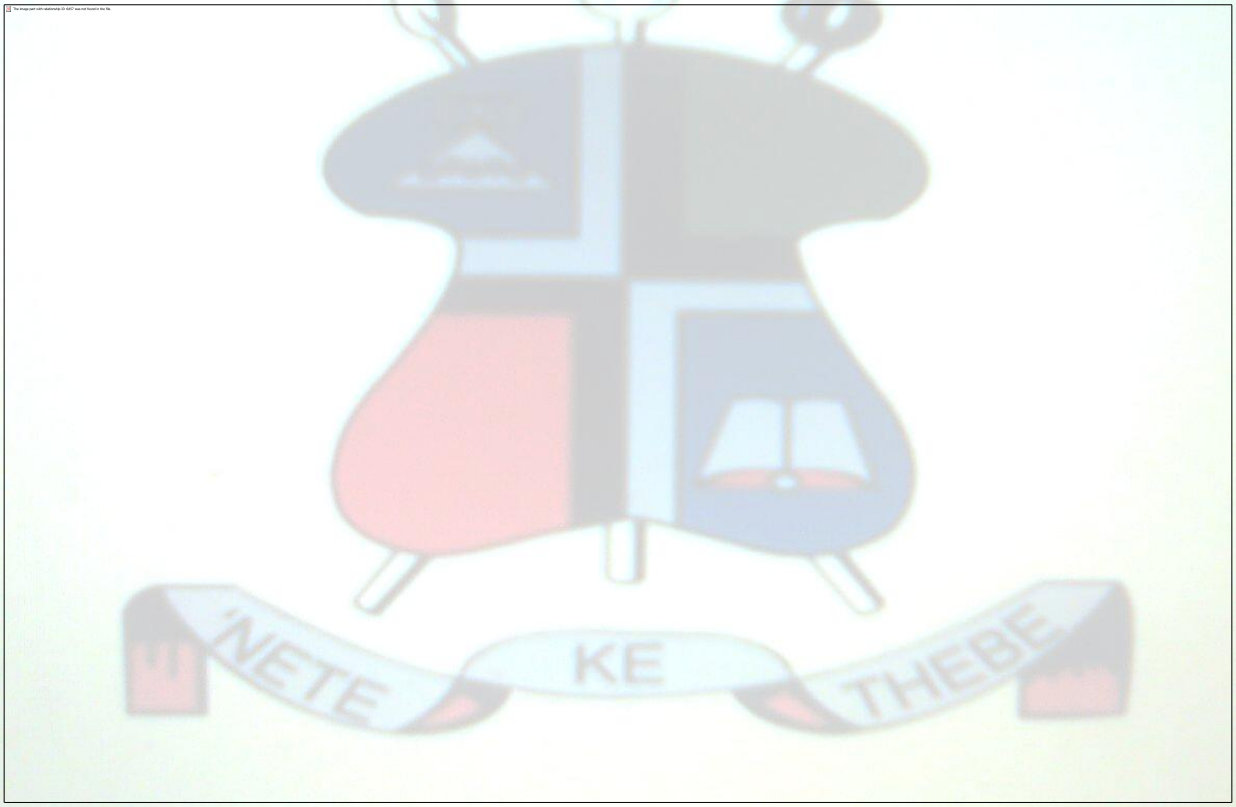

Figure 6:x-ray diffraction patterns of pure oxides and doped TiO2 NCs

4.2: Photocatalytic activity

The photocatalytic activity of all sets of composites, both SSR prepared and CPH synthesized under the visible light (λ > 420 nm; fluorescent lamp) were examined for the degradation of the CR dye. Ratio of the CR concentration at time, t, C_t to the initial CR concentration at time, t = 0 were calculated and plotted against time at 30min intervals up to 180min.

4.21: performance of chemically synthesized NCs

Fig.7 and fig 8 shows the degradation in terms of the relative percentage of CR concentration left in solution at times, 0min up to 180min as a function of time for CPH synthesized NCs in comparison with the synthesized TiO_2 for the degradation of CR. Figures 7 and 8 show the degradation curves obtained.

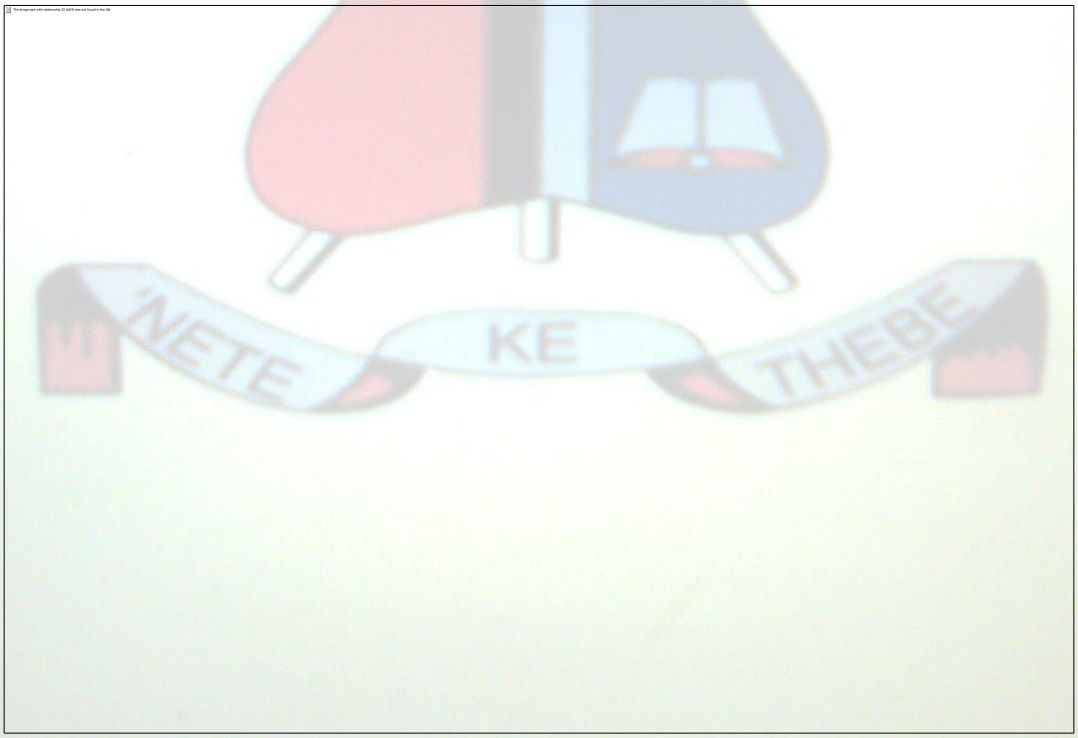

Figure 7: percentage of CR degraded within 180min with Nd2O3 doped NCs, (CPH).

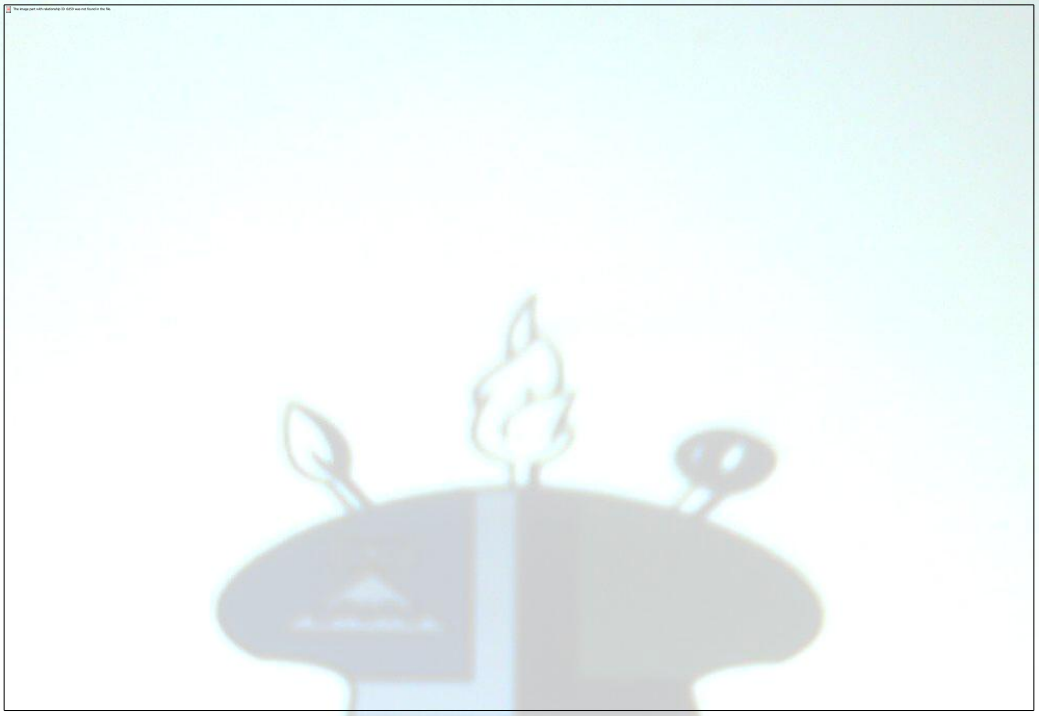

Figure 8: percentage of CR degraded within 180min with Er_2O_3 doped NCs, (CPH).

As it could be observed from figures 7 and 8, the degradation of CR dye follow exponential curve, indicating that the dye is degrading. As according to fig:7 above, it could be observed that, there is no distinct difference in photocatalytic performance between TiO_2 NCs doped with Nd_2O_3 and undoped synthesized TiO_2. Thus the photocatalytic activity of these NCs in degrading CR seems to be unchanging with increasing value of x, this is also confirmed also by the determined apparent rate constants (k_{obs}) values (28×10^{-3} min^{-1} and 27×10^{-3} min^{-1}) in figure 10. Since the performance of the synthesized TiO_2 ($k_{obs}=28 \times 10^{-3}$ min^{-1} from fig.11) is apparently the same as the performance of those doped NCs, this behavior does not show greater necessity for doping.

Fig:9 shows the degradation of CR with Er_2O_3 doped TiO_2 NCs and in this plot, it could be observed that initially the photocatalytic performance of the synthesized TiO_2 is intermediate between that of the doped NCs, however the final CR degraded within 180min is the same for synthesized TiO_2 and x=0.2 doped NCs.

The degradation rates were determined to be first order for all the sets of prepared photocatalyst, both SSR prepared and CPH NCs as well as for the synthesized TiO_2. The apparent rate constant (k_{obs}) for the degradation process was estimated from a least-square regression plots of $\ln[(C/C_o]$ as a function of time in which the negative of the slope gives the apparent rate constant. Figures 9,10 and 11 illustrate typical plots for determination of apparent rate constants for the Erbium oxides doped NCs of TiO_2 prepared by CPH and synthesized TiO_2 respectively.

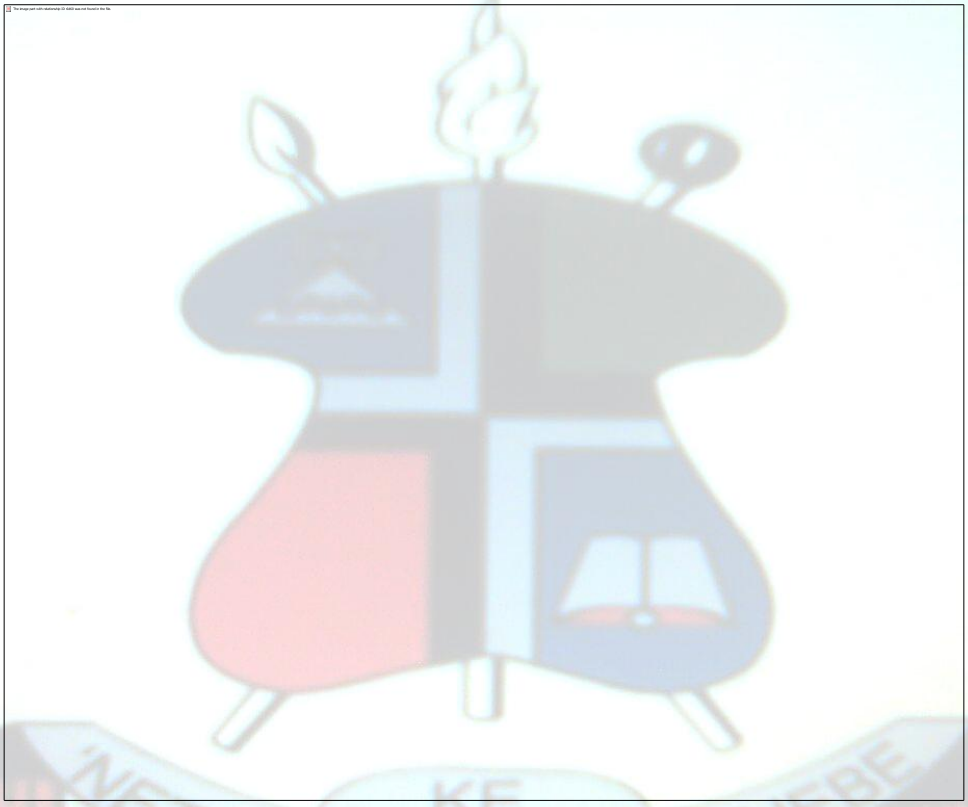

Figure 9: apparent rate constants for Er_2O_3 doped NCs in CR degradation, (CPH).

Figure 10: apparent rate constants for Nd_2O_3 doped TiO2 NCs in CR degradation, (CPH).

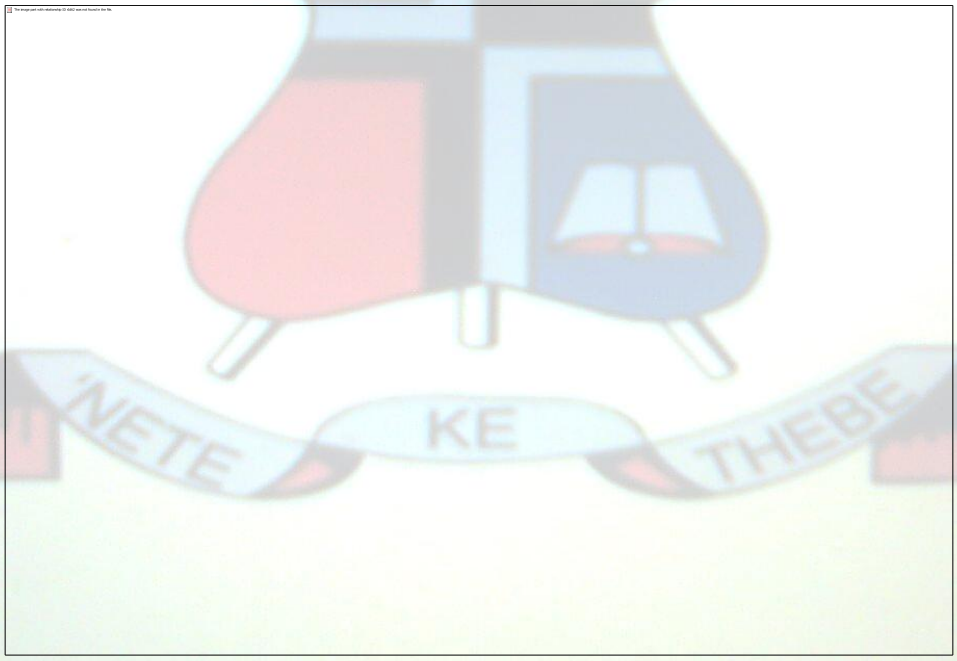

Figure 11: apparent rate constant for synthesized TiO2 NCs in CR degradation.

4.21: performance of polycrystalline NC samples prepared by SSR

Fig.12 shows the degradation curves for SSR prepared NCs in comparison with the synthesized TiO_2.

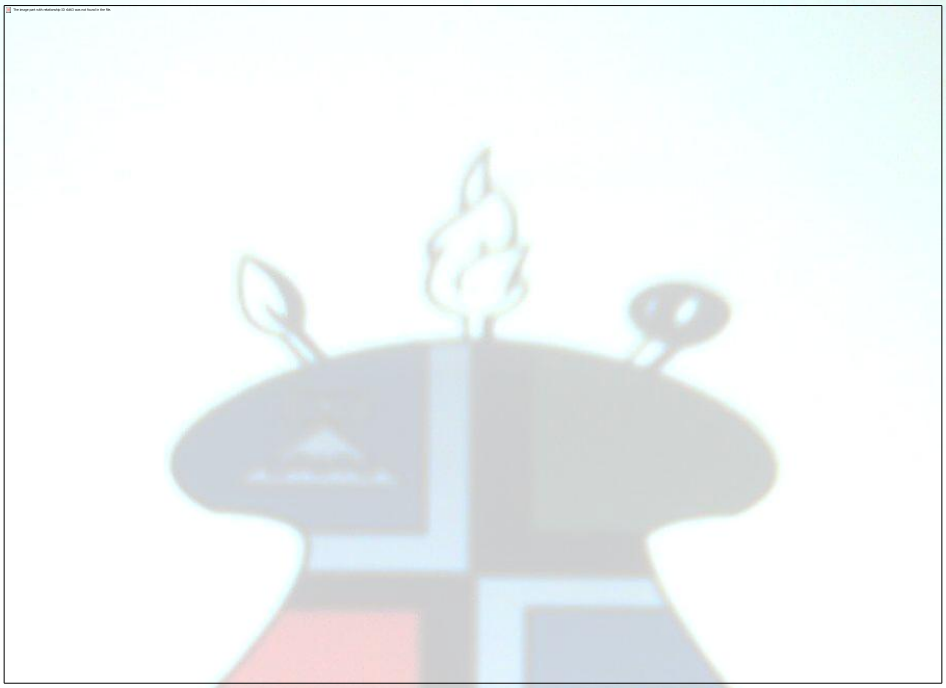

Figure 12: percentage of CR degraded within 180min with SSR doped NCs,(SSR)

From fig:12, it is observed that in all SSR prepared NCs, the photocatalytic activity increases with increasing value of x for the doped NCs, however their activities seem to be lower than for the synthesized TiO_2, this is further emphasized by the rate constants in fig:13 and fig 14. This observation reflects that doping using SSR method offer no significant improvement on photocatalytic activity of TiO_2, however this is apparently so, since the SSR prepared NCs were prepared using commercial TiO_2 but are here compared with synthesized TiO_2 which is prepared by CPH method, thus yields of differing particle sizes may be the reason which directly influence the performance. It could also be seen that fluctuations are occurring in the degradation curves which could be an implication of high suspension due to small particles which could not be illuminated by centrifugation.

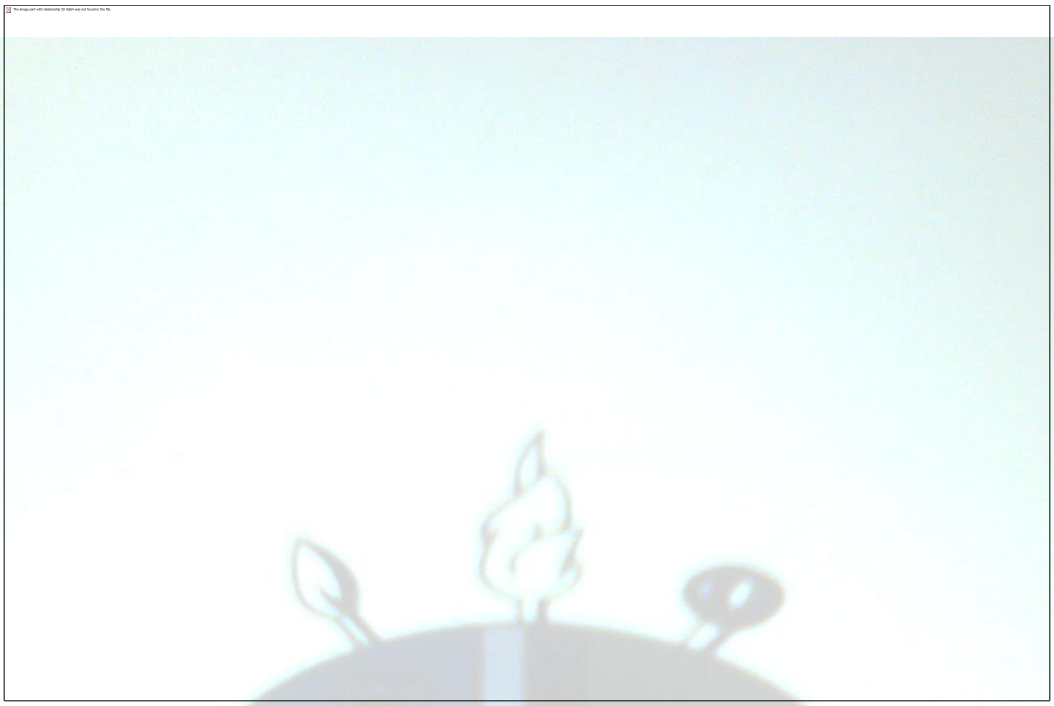

Figure 13: Apparent rate constants for Er_2O_3 doped TiO2 NCs in CR degradation, (SSR).

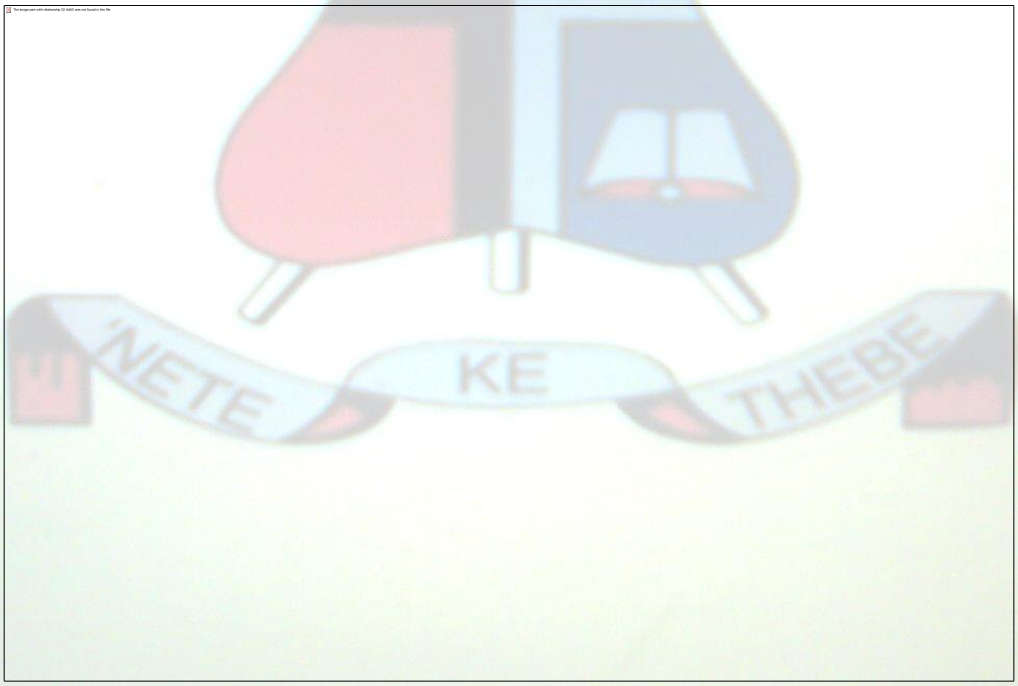

Figure 14: Apparent rate constants for Nd_2O_3 doped TiO2 NCs in CR degradation, (SSR).

Table 1: Summary of total percentage amount of CR degraded over 180min and the apparent rate constants of all NCs prepared.

Summary of results			
Sample	Fraction of dopant (*x*)	Apparent rate constants k_{obs} (x10^{-3}) min^{-1}	Degradation in 180min
CPH $TiO_2.[Nd_2O_3]_x$	0.1	28	97.4%
	0.2	27	99.6%
CPH $TiO_2.[Er_2O_3]_x$	0.1	6	89.7 %
	0.2	18	99.2%
SSR $TiO_2.[Nd_2O_3]_x$	0.1	4	64.3%
	0.2	8	85.8%
SSR $TiO_2.[Er_2O_3]_x$	0.1	2	43.8%
	0.2	4	54.5%
Synthesized TiO_2	-	28	99.6%

Generally it could be deduced from table.1 that CPH synthesized NCs have got a higher photocatalytic performance in terms of both the apparent rate constants as well as the total amount of CR degraded over 180min. this may be attributed to small particle sizes and effective doping which reduces EHP recombination [15-19], however in comparison with the synthesized TiO_2 NCs, they really do not exhibit any significant improvement on the photocatalytic efficiency of TiO_2 in degrading CR.

The SSR prepared NCs exhibit very low photocatalytic performance compared to the synthesized TiO_2, however they reveal a general trend that the photocatalytic activity of the SSR prepared NCs increases with the increasing value of x for both Erbium and Neodymium oxides doped NCs. Assuming that the effectiveness of doping determine the photocatalytic activity, it could be also deduced from table.1 that the proper and more efficient doping is achievable through chemical/CPH synthesis method than the SSR preparation method. The low activity of SSR prepared NCs may be attributed to their large particle size.

5.0 CONCLUSION AND RECOMMENDATION

Visible light photocatalytic activity of all the sets of prepared NCs of TiO_2, both Erbium oxide and Neodymium oxide doped were investigated for their photocatalytic degradation of CR dye. All the NCs synthesized by CPH method reveal better photocatalytic activity both in terms of percentage CR concentration degraded over 180min (maximum CR degraded = 99.6%) as well as the apparent rate constants than those NCs prepared by SSR method. This gives an implication that, better degradation activity of NCs is achieved through CPH than SSR, and thus for those NCs synthesized by CPH method, it concluded that they attained optimal particle size than the SSR prepared NCs. This behavior also reflects that photosensitization is the major route by which TiO_2 NCs operate in photocatalysis. On comparison with the results obtained with the synthesized TiO_2 on CR degradation, there is no evident necessity of doping since the amount of CR degraded using the synthesized TiO_2 is the same (maximum CR degraded=99.6%) as for those better performing doped TiO_2 NCs, however this is apparent since synthesized TiO_2 was also synthesized using method of Precipitation followed by hydrolysis. This also strengthens the importance of photosensitization in heterogeneous photocatalytic degradation of pollutants.

The synthesized NCs may indeed be used to reduce high organic effluents especially the synthetic dyes from industries and the ordinary sun may be used as the source of radiation to minimize costs. For the purpose of this study further work still need to be done to investigate recoverability of the photocatalyst as well as the effect on their performance after being reused.

6.0 REFERENCES

1. Bhoi K.S (2010). Adsorption Charecteristics of congo red onto PAC and GAC. Department of chem.eng. National institute of Technology,Rourkela, India.

2. Raphael B.M, Eduardo B.A and Lucia R.R (2009). Heterogeneous photocatalytic degradation of reactive dyes. Chemical engineering journal. Vol 149.

3. Souza R.R, Bresolin I.T.L, Gimenes M.L and Dias Filho B.P (2004). The performance of A fluidized bed reactor in treatment of waste water with high organic load, Brazil, journal of chem..eng, vol 2.

4. Garbai.P, Mehri A and Tabatabaii (2008). Removal of congo red fromtextile wastewater By ozonation. Int.J. Environ.Sci.Tech, vol 5, 495-500.

5. Dennis.W and Russell.R (2008). Indigo dye waste recovery from denim textile effluent. New journal of chemistry, material research and technology, university of Texas, USA. Vol 32, 2189-2184.

6. Narayan .H and Alemu .H (2009). Advances in nanotechnology. Nova science publishers Inc.
7. Steensma D.P (2001). Congo red archieves of phathology and Laboratory medicine. Accessed from http//www.en.wikipedia.org. Date 26/09/2010.

8. Tepalad T, Neramittagapong A, Neramittagapong S and Boonmee M (2008). Degradation of Congo red by ozonation. Chiang Mai journal of science, Vol 35, 63-68.
9. Karna W, Eko .S, Fatimah. I, Sri. S, Diyan. K (2006). Zeolite degradation of congo red. Vol 11, No.3, 199-209.
10. Woermer D.L (undated). Membrane technology in textile operations. Koch membrane Systems. Wilmington, MA.

11. Naeen K. and Ouyang. F (2010). Preparation of iron(III)-doped TIO_2 nanoparticles and Its photocatalytic activity under UV light. Vol 405. No.1, 221-226.

12. Narayan H, Alemu H, Macheli L, Sekota M, Thakurdesai and Gundu Rao T K (2009). Role of particle size in visible light photocatalysis of congo red. Bull. Mater, sci. Vol 32, No.5, 1-8. IOP Publishing Ltd. UK.

13. Akihiko. K, Hideki. K, Issei. T (2004). Strategies for the development of visible light Driven photocatalysis for water splitting. Chem.. letter. Vol 33, No.12, 1534.

14. Yao. Y.Y, Li. G, Ciston.S, Leuptow R.M and Gray. K (2008). Photoreactive TiO_2/ Carbon nanotubes composites; synthesis and reactivity. Enviro.Sci and Tech. vol 42, 4952-4957.

15. Fushishima. A, Rao T.N and Tryk D.A (2000). Journal of photochemistry and Photobiology. Review 1, 1-5.

16. Fabbri. D, Prevot A.B and Paramauro (2006). Application of catalysis. Bio environmental Journal. Vol 62, 21-22.

17. Linsebigler A.L, Lu. G and Yates. J.T (1995). Photocatalysis on TIO_n surfaces, principles, mechanisms and selected results. department of chemistry, university of Pittsburgh. Vol 95. 735-758.

18. Gray A.K (undated). Basic principles of photocatalysis. North wester university, USA.

19. Zhijie. L, Wenzhong. S, Wenser. H and Xiaotao (2008). Journal of hazardous materials. Vol 155, No.15, 590-594.

20. Liqiang J, Xiaojun S, Baifu. X, Baiqi. Weimin.S and Hoggang. F (2004). Journal of solid State chemistry. Vol 177, No 10, 3375-3382.

7.0 APPENDIX

7.1 Absorbance obtained using CPH synthesized NCs during CR degradation.

(λ=496nm-499nm)

Time	Absorbance	C/C_o (%)	$\ln[C/C_o]$
0	0.233	100	0
30	0.074	31.8	-1.147
60	0.051	21.9	-1.519
90	0.048	20.6	-1.560
120	0.041	17.6	-1.737
150	0.033	14.2	-1.954
180	0.024	10.3	-2.273

$TiO_2[Er_2O_3]x=0.1$

time	Absorbance	C/C_o (%)	$\ln[C/C_o]$
0	0.254	100	0
30	0.035	13.8	-1.981
60	0.01	3.94	-3.235
90	0.008	3.15	-3.458
120	0.007	2.76	-3.591
150	0.003	1.18	-4.439
180	0.002	0.79	-4.844

$TiO_2[Er_2O_3]x=0.2$

Time	Absorbance	C/Co (%)	$\ln[C/C_o]$
0	0.233	100	0
30	0.072	30.9	-1.174
60	0.015	6.4	-2.742
90	0.011	4.7	-3.053
120	0.006	2.6	-3.659
150	0.006	2.6	-3.659
180	0.006	2.6	-3.659

$TiO_2[Nd_2O_3]x=0.1$

time	Absorbance	C/C_o (%)	$\ln[C/C_o]$
0	0.25	100	0
30	0.062	24.8	-1.394
60	0.027	10.84	-2.222
90	0.018	7.2	-2.631
120	0.01	4	-3.219
150	0.002	0.8	-4.828
180	0.001	0.4	-5.521

$TiO_2[Nd_2O_3]x=0.2$

time	Absorbance	C/C_o (%)	$\ln[C/C_o]$
0	0.24	100	0
30	0.062	25.8	-1.353
60	0.027	11.3	-2.184
90	0.018	7.5	-2.590
120	0.01	4.2	-3.178
150	0.002	0.8	-4.787
180	0.001	0.4	-5.480

Synthesized TiO_2

7.8 Absorbance obtained using SSR Prepared NCs during CR degradation.

(λ=496nm-499nm)

time	Absorbance	C/C_o (%)	$\ln[C/C_O]$
0	0.217	100	0
30	0.19	87.6	-0.133
60	0.16	73.7	-0.305
90	0.14	64.5	-0.438
120	0.132	60.8	-0.497
150	0.129	59.4	-0.520
180	0.122	56.2	-0.576

$TiO_2[Er_2O_3]x=0.1$

time	Absorbance	C/Co (%)	ln[C/Co]
0	0.268	100	0
30	0.21	78.4	-0.243
60	0.173	64.6	-0.438
90	0.144	53.7	-0.621
120	0.131	48.9	-0.715
150	0.121	45.1	-0.795
180	0.122	45.5	-0.787

$TiO_2[Er_2O_3]x=0.2$

Time	Absorbance	C/C_o	$\ln[C/C_o]$
0	0.258	100	0
30	0.198	76.7	-0.265
60	0.161	62.4	-0.471
90	0.131	50.8	-0.678
120	0.124	48.1	-0.733
150	0.106	41.1	-0.889
180	0.092	35.7	-1.031

$TiO_2[Nd_2O_3]x=0.1$

time	Absorbance	C/C_o	$\ln[C/C_o]$
0	0.233	100	0
30	0.085	36.5	-1.008
60	0.056	24.0	-1.425
90	0.051	21.9	-1.519
120	0.038	16.3	-1.813
150	0.037	15.9	-1.840
180	0.033	14.2	-1.956

$TiO_2[Nd_2O_3]x=0.2$